

FLOW INJECTION SPECTROPHOTOMETRIC DETERMINATION OF NARINGENIN IN SUPPLEMENTS USING SOLID-PHASE REACTOR CONTAINING IMMOBILIZED MANGANESE DIOXIDE

ISRAA M JAWAD AL MASHHADANI*, SADEEM SUBHI ABED

Department of Chemistry, College of Science, University of Baghdad, Jadriyah, Baghdad, Iraq. Email: bangels_is@yahoo.com

Received: 14 May 2018, Revised and Accepted: 15 June 2018

ABSTRACT

Objective: Naringenin (NAR) is a part of the human daily diet, and it plays an important role in human health for its biological functions. This study describes a new, sensitive, simple, and accurate method for determining NAR in supplements.

Methods: The method is based on oxidative coupling reaction between NAR and N, N-dimethyl-p-phenylenediamine in an alkaline medium using manganese dioxide immobilized in cellulose acetate as online oxidant agent to form a colored product which can be monitored at λ_{max} 598 nm.

Results: Several operating parameters such as reactor column length, particles size, chemicals, and physicals reaction conditions were studied. The proposed method was sensitive and good repeatable, the linear range of NAR concentration was from 1 to 70 $\mu\text{g/ml}$ with a limit of detection of 0.292 $\mu\text{g/ml}$, and recovery range of analysis was 99.55–100.48%.

Conclusion: The proposed method was successfully applied for determining NAR in supplements.

Keywords: Naringenin, Flow injection, Spectrophotometry, Solid phase reactor, Immobilized manganese dioxide, Supplements.

© 2018 The Authors. Published by Innovare Academic Sciences Pvt Ltd. This is an open access article under the CC BY license (<http://creativecommons.org/licenses/by/4.0/>) DOI: <http://dx.doi.org/10.22159/ajpcr.2018.v11i8.27292>

INTRODUCTION

Naringenin (NAR) is a white powder, soluble in organic solvents. Its chemically name is (2, 3-dihydroxy-2-(4-hydroxyphenyl)-4H-1-benzopyran-4-one, with molecular weight of 272.3 g/mol) [1]. NAR (Fig. 1) can be found in citrus fruits, beverages, and vegetables [2]. It can exhibit a wide range of biological properties: Antioxidant, antimicrobial, antiviral, anti-allergic, antiestrogenic, antidiabetic, anti-inflammatory, anti-obesity, anticancer activity, enzymes inhibitor and lowering cholesterol, and blood lipid reduce low-density lipoprotein [3- 6]. It has been reported that NAR has been determined in fruits [7], honey [8], human urine and plasma [9].

Different analytical methods were used to determine NAR, such as high-performance liquid chromatographic [10,11], capillary electrophoresis CE coupled to ultraviolet (UV), capillary electrophoresis coupled to mass spectrometry with an electrospray interface (CE-ESI-MS) [12], capillary zone electrophoresis [13], and gas chromatographic (GC) with MS [14].

Solid-phase reactors (SPRs) were used in flow injection analysis (FIA) manifold to offer many advantages such as reducing reagents consumption, reducing waste generation, simplified manifold, increase the sensitivity, and increase the samples throughput [15]; therefore, numerous FIA systems with SPR have been reported for pharmaceuticals analysis [16-18].

In the present study, SPR incorporated in flow injection manifold was utilized for the determination of NAR, knowing that no SPR coupled to reverse flow injection manifold (r FIA) has been reported for determining NAR. The determining method based on using SPR contains manganese dioxide immobilized on cellulose acetate (SPR- Mn) as oxidant agent in the oxidative coupling reaction between NAR and N,N-dimethyl-p-phenylenediamine dihydrochloride (DMPD) in sodium hydroxide medium to form colored product can be detected spectrophotometrically.

METHODS

Apparatus

Digital double-beam recording spectrophotometer (Shimadzu UV-VIS 260, Kyoto, Japan) was used for spectral and absorbance monitored for NAR determination, flow cells (Cecil) of 1 cm path made of quartz with 50 ml internal volume, 6-ways injection valve (Knauer, Germany) with various sample loops, peristaltic pump (Shenzhen, China) was used to transport the carrier solution, flexible portly vinyl chloride tubes of 0.8 mm internal diameter was used for the peristaltic pump, and flexible Teflon tubes of 0.5 mm internal diameter was used for reaction coils and to transport the reagents solutions. Sieves (50×200 mm) of different mesh size (Retsch GmbH and Co., KG, Germany) used to get the suitable particles size.

rFIA manifold and procedure

Fig. 2 shows the rFIA manifold used in this work. 100 μl of 5×10^{-3} M of DMPD was injected into a stream of 0.3 M NaOH (the carrier solution) through the injection valve at a total flow rate of 1.95 ml/min. The reagent (DMPD) oxidized through SPR-Mn and then combined at T-link with a stream of NAR (1–70 $\mu\text{g/ml}$). After complete mixing in the 50 cm reaction coil, the absorbance was measured at 598 nm at room temperature (25°C).

Reagents, chemicals, and supplements

Chemicals and reagents used in this work were of analytical grade.

NAR

NAR (NAR, 500 $\mu\text{g/ml}$) was supplied from Carl Roth, Germany: Stock solution was prepared daily by dissolving 0.05 g of NAR in 100 ml of ethanol; working solutions were prepared by suitable dilution of the stock with distilled water.

DMPD

DMPD (0.01 M) was freshly prepared by dissolving 0.1045 g of DMPD (209.12 g/mol, BDH, England) in 50 ml distilled water. The prepared solution was kept in a brown bottle.

Sodium hydroxide solution

Sodium hydroxide solution (1 M) was prepared by dissolving 20 g of sodium hydroxide (40 g/mol, BDH, England) in distilled water and then transferred into 500 ml volumetric flask and diluting to the mark with the same solvent.

Supplements samples (500 µg/ml)

An appropriate number of supplements capsules (Alternative Medicine Solutions, Inc., USA, 250 mg) were emptied and weighted, and the average weight of the content of one capsule was taken. An accurate weight equivalent to 0.05 g of NAR was taken and dissolved in ethanol into a 100 ml volumetric flask; the residue was washed with ethanol, completed to the mark with the same solvent, and then filtered. More diluted solutions were prepared by simple dilution with distilled water.

Preparation of Mn-SPR

The immobilization of MnO_2 was similar to that previously reported [19], 0.25 g cellulose acetate (CA) was completely dissolved in 0.5 ml dimethylformamide and 3 ml acetone while stirring, and 4 g manganese dioxide powder was added slowly to the solution. The mixture was homogenized by manual stirring until an obvious increase in viscosity 10 min later, the mixture was washed with distilled water and rigid polyester (solid) was obtained and left for air-drying. After drying the polyester (containing immobilized MnO_2) breaking, cutting and sieving steps carry out to get 1.0 mm particles size. The SPR was constructed from glass tubing (2 mm i.d. and 6 cm length); the tubing was packed with 0.1502 g of 1.0 mm particles. Small pieces of sponge insert at the ends of the tube to hold the particles in place. SPR placed to the manifold between the injector valve and the detector. The packing reactor conditioned for at least 10 min before use by passing distilled water and then passing the carrier solution to minimize the particles compaction in the reactor.

RESULTS AND DISCUSSIONS

Absorption spectra

The absorption spectra of the colored product was obtained by carrying out the reaction in 10 mL volumetric flask. A 40 µg/ml of NAR, 1 ml of 5×10^{-3} M of DMPD, 0.1 g of immobilized MnO_2 and 1 ml of 0.3 of NaOH were mixed and swirled. The blue colored product was formed immediately, the solution was diluted with distilled water to the mark and then filtered. The absorption spectra were recorded between 350 and 1100 nm, and maximum absorbance was recorded at 598 nm against reagent blank which has neglected absorbance at this wavelength (Fig. 3).

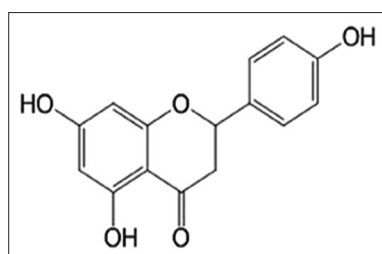


Fig. 1: Structure of naringenin ($C_{15}H_{12}O_5$)

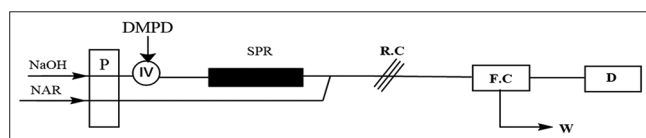


Fig. 2: Schematic representation of r flow injection analysis manifold; I.V: Injection valve, P: Peristaltic pump, FC: Flow cell, D: Detector, SPR: Solid-phase reactor containing immobilized MnO_2 , and W: Waste

The probable mechanism for the coupling reaction of NAR and DMPD is depicted in Scheme 1. The oxidant (MnO_2) led to oxidize DMPD which loses two electrons and a proton to yield diethyl benzoquinone-diimine [20], and this reactive compound couples with NAR by the electrophilic attack at their nucleophilic site, at slightly alkaline medium, if possible at para-position of NAR.

Different parameters which influenced the absorbance intensity including SPR- parameters and chemical and physical conditions were studied and optimized by altering one variable in time while keeping others constant. The experiments were carried out using 40 µg/mL of NAR, three injections were performed, and the average absorbance was taken.

SPR parameters

The SPR containing manganese dioxide has essential roles in the proposed method, and it is not only responsible for DMPD oxidation into the active compound but also responsible for the dispersion of reactant plug in the flow system. Several factors influencing the reactor performance, such as MnO_2 :polymeric resin ratio, reactor length, particles weight, and particles size, were studied.

To investigate the suitable ratio of immobilized MnO_2 in the matrix (CA), different ratios were used in SPR preparation. The high sensitivity and reproducibility were obtained with the ratio (4: 0.25); thus, this ratio was adopted in the next experiments (Fig. 4a).

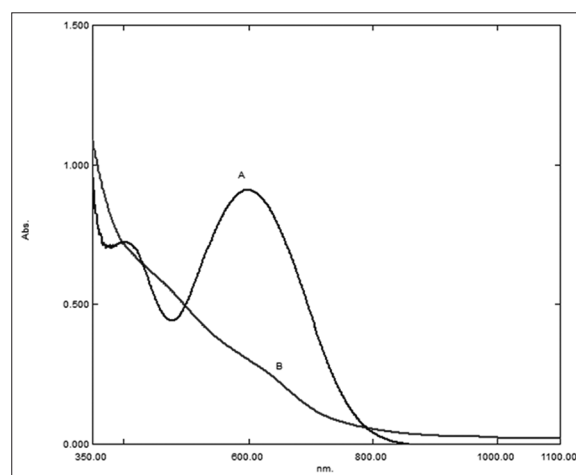
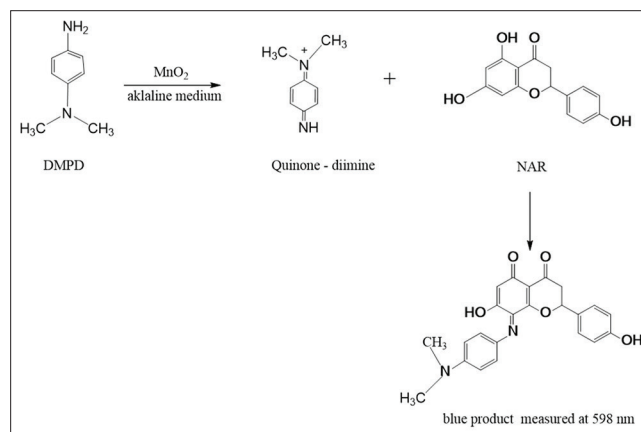


Fig. 3: The absorption spectra of the blue product against the reagents blank (A), reagents blank against distilled water (B)



Scheme 1: The probable reaction mechanism between naringenin and N,N-Dimethyl-p-phenylenediamine dihydrochloride

Particle size influence was studied in the range of 0.15–1.18 mm mesh (the column was packed with the same weight for each study). With the increasing of the size of particles up to 1 mm, the absorbance was also increased, and the smaller particle size leads to high hydrodynamic resistance and lower sampling rate; therefore, 1 mm was used in further experiments as a compromise between sensitivity and the sampling frequency (Fig. 4b).

Testing the reactor length and particle weight was carried out with different lengths of reactors in range (4–12 cm) and packed with different particles weight from 0.0775 to 0.2012 g, as Fig. 4c and d shows that the maximum absorbance and stability of baseline were obtained when 6-cm column length packed with 0.1502 g of particles; the reactor shorter than 6 cm led to lowering the residence time, while the reactor higher than 6 cm increased the dispersion. In respect to the particles weight, it was found that the strong backing (weight above 0.1502 g) leads to increase the resistance against the flow stream, and hence, the reactor of 6 cm packed with 0.1502 g selected as the optimum reactor.

Chemical and physical parameters

The variables that influenced rFIA performance were studied to choose the variables which gave the best absorbance, sample throughput, reproducibility, and longer life-span of SPR.

Varying concentration of DMPD in the range (1×10^{-3} to 9×10^{-3} M) was studied to examine the reagent effect on the reaction. Maximum absorbance was obtained when the concentration of DMPD was 5×10^{-3} M, so this concentration was chosen for further use (Fig. 5).

The preliminary tests indicated that the alkaline medium leading essential for developed the color product, and for that therefore, the reaction was performed in the presence of 0.2 M of sodium carbonate, sodium hydroxide, ammonium hydroxide, and potassium hydroxide to select the suited base solution. It was found that using sodium hydroxide gave the maximum sensitivity of the product the concentration of sodium hydroxide was optimized, and the results are shown in Fig 6a and b indicated that 0.3 M was the optimum concentration and used from here on.

Under the optimal reagent and base concentrations, physical flow parameters were experienced to obtain the compromise between absorbance, sample throughput, and reproducibility. Sample volume,

reaction coil length, and total flow rate were studied in separated experiments.

The total flow rate was tested in the range of 0.2–3.2 ml/min. When flow rate reached to 1.95 ml/min, best sensitivity obtained, and above this flow rate, it was found that the sensitivity decreased because of both dilution and the reaction incomplete; nevertheless, the lower flow rate increased the analysis time and decreased the sample rate. The flow rate of 1.95 ml/min was chosen for further use to balance the sensitivity and the sample throughput.

Effect of the reaction coil length on the absorbance and sampling rate was investigated using different reaction coil lengths in the range of 0–200 cm; 50 cm gave the maximum absorbance. Using longer coil, length causes a decrease in absorbance because of the increase in dispersion; therefore, 50 cm reaction coil was selected. The influence of the sample volume was studied in 75–250 μ l range. It was found from this study that using 100 μ l sample loop gave the best absorbance signal, in addition to the reduced in reagent consumption. Fig. 7 shows the results obtained from the study of physical parameters.

Under the optimum reaction conditions, the sample throughput was 60 samples per hour, and reactor lifetime and reproducibility were also investigated. The SPR material found stable for more than 40 days, and reactor preparation's reproducibility was good (for 37 injections, the relative standard deviation was [RSD %] = 2.38 and for more than 45 injections, RSD% <5).

Analytical characteristics

The calibration curve was obtained by plotting the absorbance versus the corresponding concentrations. Under the optimum conditions, series of solutions containing 1–70 μ g/ml of NAR in 10 ml volumetric flasks treated as the proposed procedure. Table 1 summarizes the analytical characteristics values. The accuracy and precision of the proposed method were studied under the optimum conditions using different concentrations of NAR, and the results obtained show good accuracy and precision based on the values of the relative error (E %) and RSD %, (Table 2).

Evaluation of the proposed method

To assess the quality and validity of the determination method of NAR, a comparison was made between the proposed analytical method and

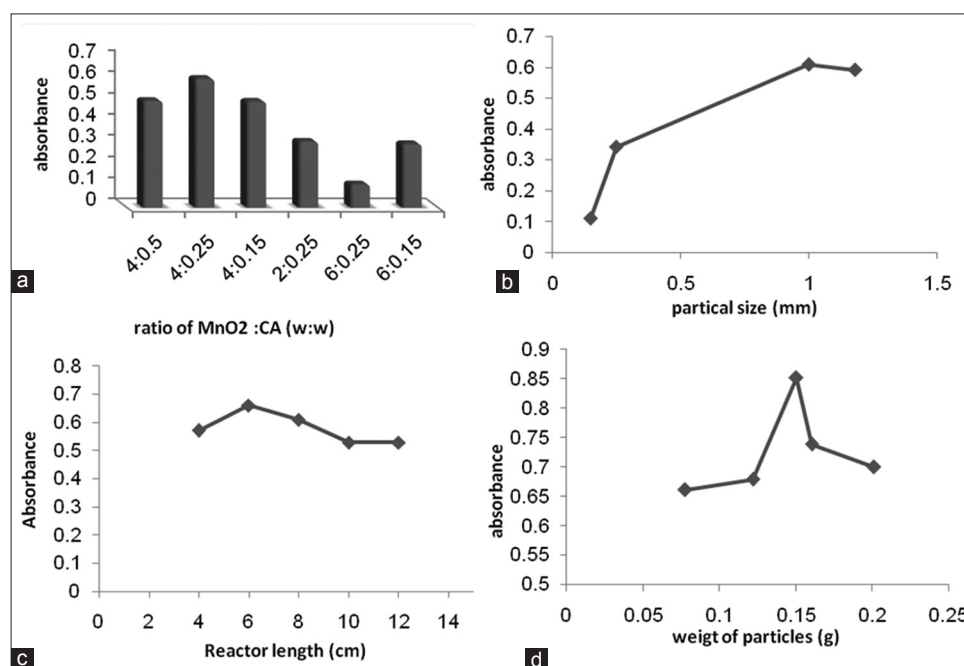


Fig. 4: Effect of solid phase reactors parameters (a) MnO₂:cellulose acetate ratio, (b) particles size, (c) reactor length, (d) particles weight

the reported UV method [21]. NAR was analyzed using UV-vis 260 Shimadzu double-beam spectrophotometer, the spectrum of 15 µg/ml of NAR in ethanol was traced between 200 and 600 nm against reagent blank of ethanol, and it was found that maximum absorption was at a wavelength of 292 nm (Fig. 8). Calibration graph was constructed, and the linear range for UV method was 0.5–30 µg/ml of NAR concentration.

This method was applied for determining NAR in supplements, an accurately weighed of contents of 10 capsules powder equivalent to 0.01 g of pure NAR was dissolved in ethanol and transferred into 100 ml volumetric flask, and the volume was completed to the mark with ethanol and then filtered to obtain 100 µg/ml of NAR. More diluted solutions were prepared by simple dilution with ethanol to get 5, 7, and 15 µg/ml of NAR; the absorbance was measured at λ_{max} of 292 nm against the reagent blank.

Application analysis and recovery

The standard addition method was applied to exclude the effect of the interferences; this test was performed by spiking the pure sample with

Table 1: Analytical values of the proposed method for NAR determination

Parameter	Value
Regression equation	Y=0.0213x+0.0179
Correlation coefficient, r	0.9993
Linear concentration range (µg/ml)	1–70
Molar absorptivity (L/mol/cm)	5799.138
Sandell's sensitivity, S (µg/cm)	0.0470
Standard deviation of the residuals, $S_{y/x}$	0.0088
Standard deviation of the slope, S_b	0.000126
Standard deviation of the intercept, S_a	0.0049
Limit of detection (µg/ml)	0.292
Limit of quantification (µg/ml)	0.973
RSD %	1.303

NAR: Naringenin, RSD: Relative standard deviation

Table 2: Accuracy and precision of the proposed method for the determination of NAR

Concentration of NAR µg/ml	E%	Rec. %	RSD %
20	-0.445	99.555	1.236
30	+0.486	100.486	1.557
40	-0.340	99.660	1.118

*Average of three determinations. NAR: Naringenin, RSD: Relative standard deviation

Table 3: Recovery test using standard addition method

Supplements	Concentration of NAR µg/ml		E%	Rec. %	RSD %
	Present	Found*			
Naringenin capsule 250 mg (alternative medicine solutions Inc., USA)	5	5.025	+0.500	100.500	1.971
	10	10.088	+0.880	100.880	1.251
	20	20.089	+0.445	100.445	1.229

*Average of three determinations. NAR: Naringenin, RSD: Relative standard deviation

three different concentrations of NAR supplements. The result obtained was indicating good accuracy and precision (Table 3).

The proposed method was also applied to determinate NAR in capsule supplements directly. Three concentrations were analyzed using previous optimal conditions. The results are compared statistically with those obtained using UV method [21] using t-test and F test at 95% confidence level [22]. In terms of accuracy and precision, the results indicate that there was no significant difference between the proposed method and the comparative method (Table 4).

Table 4: Analytical results of the application the proposed method for the determination of NAR in supplements directly

Supplements	Proposed method				Classical method
	Conc. of NAR µg/ml				
	Present	Found*	RSD %	Rec. %	
Naringenin capsule 250 mg (alternative medicine solutions)	10	10.098	1.010	100.980	100.572
	20	20.145	1.500	100.725	100.227
	30	29.989	1.750	99.963	
Pure NAR	1.303			99.900	
$t=(4.303)$ **0.464 $F=(161.4)$ *3.615 $n_1-1 = n_2-1 = 1$					

*Average of three determinations. **Theoretical value. NAR: Naringenin

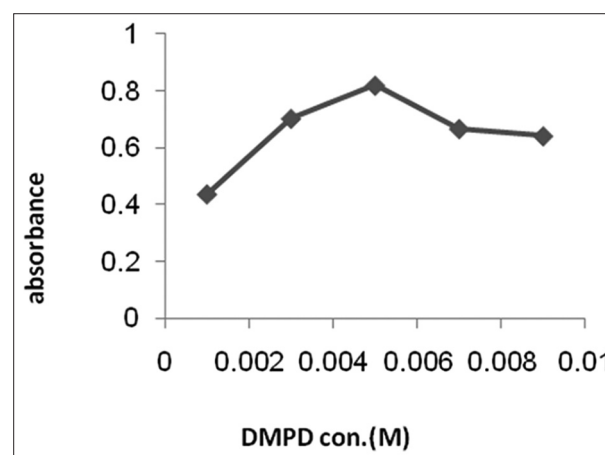


Fig. 5: Effect of concentration of N,N-dimethyl-p-phenylenediamine dihydrochloride

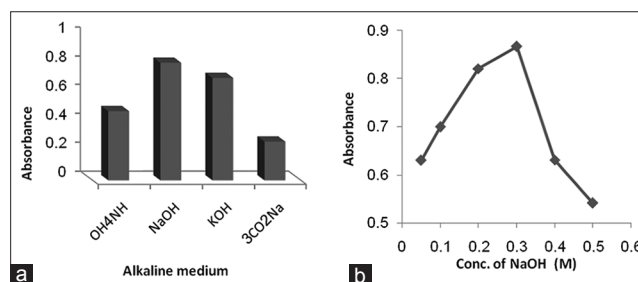


Fig. 6: (a) Effect of alkaline medium type, (b) effect of NaOH concentration

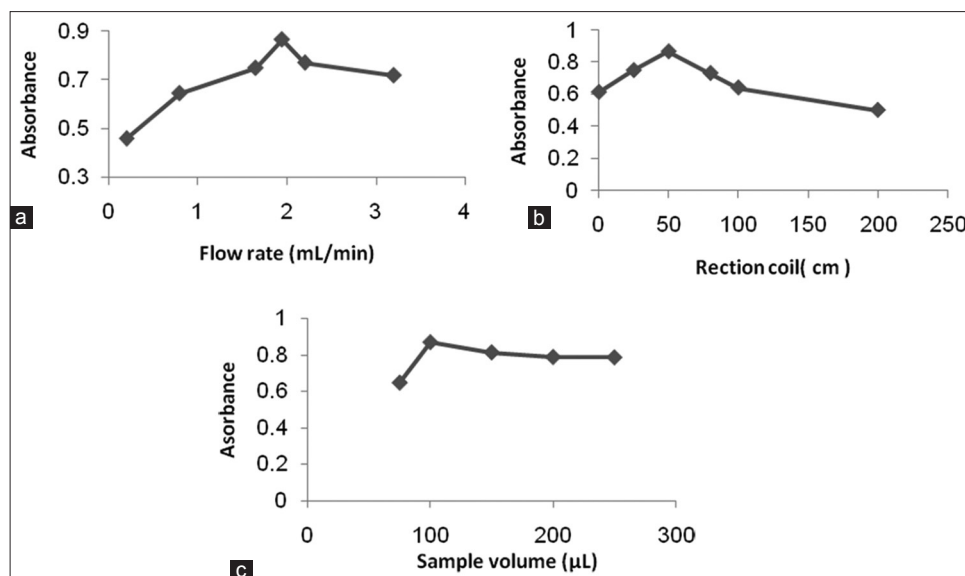


Fig. 7: Physical parameters optimization: (a) Effect of flow rate, (b) effect of reaction coil, (c) effect of the sample loop

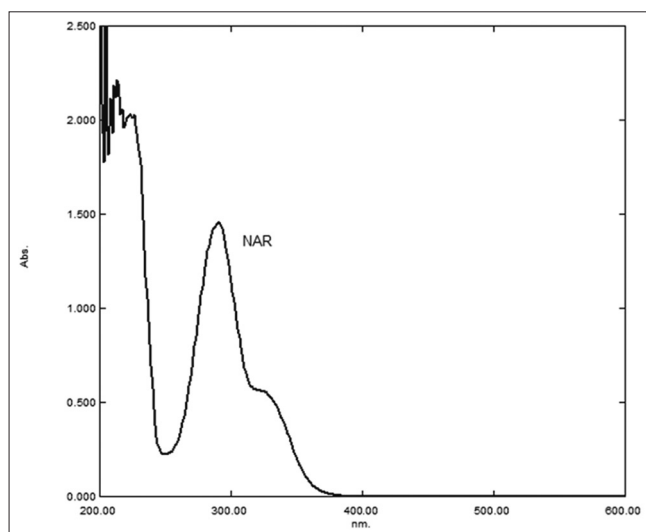


Fig. 8: Absorption spectrum of 15 $\mu\text{g/ml}$ of naringenin in ultraviolet region

CONCLUSION

This study demonstrated the ability of determining NAR in supplements depending on the oxidative coupling reaction between NAR and the reagent N, N-dimethyl-p-phenylenediamine in alkaline medium with online SPR containing immobilized MnO_2 as oxidant. The proposed rFIA is sensitive, safe, cost-effective, and good sample throughput (60 samples per hour) to allow the determination of NAR in supplements. Moreover, the reactor material was stable for a long time. The results obtained were compared with the reported UV method, the comparison indicated clearly that there is no significant difference between the proposed method and the reported method, and the proposed method could be recommended for routine determination of NAR in pure and supplements form.

AUTHOR'S CONTRIBUTION

All authors have contributed equally.

CONFLICTS OF INTEREST

Authors have no conflicts of interest

REFERENCES

1. Seridi L, Boufelfel A. Naringenin encapsulation in β -CD and in heptakis (2, 6-di-O-methyl)- β -CD: NMR, NBO and QTAIM analysis. *J Incl Phe Macrocycl Chem* 2018;87:287-304.
2. Al Harbi M. Hepatoprotective effect and antioxidant capacity of naringenin on arsenic-induced liver injury in rats. *Int J Pharm Pharm Sci* 2016;8:103-8.
3. Al Juhaimi F, Özcan MM, Uslu N, Ghafoor K. The effect of drying temperatures on antioxidant activity, phenolic compounds, fatty acid composition and tocopherol contents in citrus seed and oils. *J Food Sci Technol* 2018;55:190-7.
4. Isobe T, Ohkawara S, Ochi S, Tanaka-Kagawa T, Jinno H, Hanioka N. Naringenin glucuronidation in liver and intestine microsomes of humans, monkeys, rats, and mice. *Food Chem Toxicol* 2018;111:417-22.
5. Luis Á, Duarte AP, Pereira L, Domingues F. Interactions between the major bioactive polyphenols of berries: Effects on antioxidant properties. *Eu Food Res Technol* 2018;244:175-85.
6. Ab K, Sh J, Sh PP. Effect of naringenin on lipids, lipoproteins and lipid metabolising enzymes in 7,12-Dimethylbenza(A) anthracene-induced mammary carcinogenesis in SD rats. *Int J Pharm Pharm Sci* 2016;8:154-8.
7. Arruda HS, Pereira GA, de Moraes DR, Eberlin MN, Pastore GM. Determination of free, esterified, glycosylated and insoluble-bound phenolics composition in the edible part of araticum fruit (*Annona crassiflora* Mart.) and its by-products by HPLC-ESI-MS/MS. *Food Chem* 2018;245:738-49.
8. Jasicka-Misiak I, Makowicz E, Stanek N. Chromatographic fingerprint, antioxidant activity, and colour characteristic of polish goldenrod (*Solidago virgaurea* L.) honey and flower. *Eur Food Res Technol* 2018;2018:1-6.
9. Sus N, Schlien J, Calvo-Castro LA, Burkard M, Venturelli S, Busch C, Frank J. Validation of a rapid and sensitive reversed-phase liquid chromatographic method for the quantification of prenylated chalcones and flavanones in plasma and urine. *NFS J* 2018;10:1-9.
10. Kanaze FI, Kokkalou E, Georganakis M, Niopas I. Validated high-performance liquid chromatographic method utilizing solid-phase extraction for the simultaneous determination of naringenin and hesperetin in human plasma. *J Chroma B* 2004;801:363-7.
11. Kanaze FI, Kokkalou E, Georganakis M, Niopas I. A validated solid-phase extraction HPLC method for the simultaneous determination of the citrus flavanone aglycones hesperetin and naringenin in urine. *J Pharma Biomed Anal* 2004;36:175-81.
12. Huck CW, Stecher G, Ahrer W, Stögl WM, Buchberger W, Bonn GK. Analysis of three flavonoids by CE-uV and CE-ESI-MS. Determination of naringenin from a phytomedicine. *J Sep Sci* 2002;25:903-8.
13. Andrade P, Ferreres F, Gil MI, Tomás-Barberán FA. Determination of phenolic compounds in honeys with different floral origin by capillary zone electrophoresis. *Food Chem* 1997;60:79-84.

14. Spanakis M, Kasma S, Niopas I. Simultaneous determination of the flavonoid aglycones diosmetin and hesperetin in human plasma and urine by a validated GC/MS method: *In vivo* metabolic reduction of diosmetin to hesperetin. *Biomed Chroma* 2009;23:124-31.
15. Noroozifar M, Khorasani-Motlagh M, Taheri A, Homayoonfard M. Application of manganese(IV) dioxide microcolumn for determination and speciation of nitrite and nitrate using a flow injection analysis-flame atomic absorption spectrometry system. *Talanta* 2007;71:359-64.
16. Vicentini FC, Suarez WT, Cavaleiro ET, Fatibello-Filho O. Flow-injection spectrophotometric determination of captopril in pharmaceutical formulations using a new solid-phase reactor containing AgSCN immobilized in a polyurethane resin. *Braz J Pharm Sci* 2012;48:325-33.
17. Corominas BG, Pferzschner J, Icardo MC, Zamora LL, Martínez Calatayud J. *In situ* generation of co(II) by use of a solid-phase reactor in an FIA assembly for the spectrophotometric determination of penicillamine. *J Pharm Biomed Anal* 2005;39:281-4.
18. Vakh C, Koronkiewicz S, Kalinowski S, Moskvina L, Bulatov A. An automatic chemiluminescence method based on the multi-pumping flow system coupled with the fluidized reactor and direct-injection detector: Determination of uric acid in saliva samples. *Talanta* 2017;167:725-32.
19. Zhang ZQ, Tang Y. Solid-phase reactor flow-injection on-line oxidizing spectrofluorimetry for determination and dissolution studies of folic acid. *Anal Bioanal Chem* 2005;381:932-6.
20. Sastry CS, Suryanarayana MV, Tipirneni AS. Application of p-N,N-dimethylphenylenediamine dihydrochloride for the determination of some diuretics. *Talanta* 1989;36:491-4.
21. Cordenonsi LM, Sponchiado RM, Garcia CV, Raffin RP, Schapoval EE. Study of flavonoids present in pomelo (*Citrus maxima*) by DSC, UV-VIS, IR, ¹H and ¹³C NMR and MS. *Drug Ana Res* 2017;1:31-7.
22. Miller J, Miller JC. *Statistics and Chemometrics for Analytical Chemistry*. Harlow Prentice Hall: Pearson Education; 2010.